

Multi-fidelity optimization of horizontal axis wind turbines

Michael K. McWilliam, Frederik Zahle, Christian Pavese
Jose P. A. A. Blasques, Carlo Tibaldi

This paper is concerned with the numerical design optimization of wind turbines. Many examples of wind turbine design optimization in literature rely on simplified analysis in some form. This may lead to sub-optimal design, because the optimizer does not see the full fidelity of the problem. To overcome these challenges, this research will explore the multi-fidelity Approximation and Model Management Framework (AMMF) optimization algorithm. AMMF is similar to conventional gradient based optimization, except in the search phase of the optimization, the analysis is replaced with a fast low-fidelity model that has been corrected to give C^1 consistency with the high-fidelity model. AMMF was first explored with a simple preliminary investigation based on analytic equations. Second, it was applied to a single-discipline design optimization problem to find the internal structure with the least weight. Finally, AMMF was used in full aero-elastic wind turbine rotor design optimization problem based on the DTU 10 MW reference wind turbine design. Mixed results were achieved for the final study and further work is needed to find the best configuration for AMMF.

I. Introduction

Multi-disciplinary Design Optimization (MDO) is a common practice in the preliminary design of wind turbine rotors. An early example is given by Fuglsang¹ where a Blade Element Momentum (BEM) and linear beam model was coupled to a Sequential Linear Programming (SLP) algorithm to find blade designs that minimized the Cost Of Electricity (COE).

Evaluating the loads (*i.e.* the constraints in the optimization) is one of the largest challenges in wind turbine MDO. First, to adequately evaluate the loads for certification, typically 1880 unsteady simulations are required to simulate 259 hours of operation.^{2,3} Hjort *et. al.*⁴ developed an optimization framework that included wide scope of disciplines and included many of the Design Load Cases (DLCs) within the optimization. To obtain results in a reasonable amount of time, they had to rely on massively parallel clustered computing resources. This approach is expensive and not widely feasible to the general wind energy community.

To overcome this challenge, many researchers turn to simplifications. The original work by Fuglsang *et. al.* used steady state analysis and simple load extrapolation method tuned by unsteady simulations. The work of Bottasso⁵ extended this method with a bi-level optimization framework for aero-servo-elastic design optimization. At the lower level an optimization algorithm explored the design space with steady-state simulations. Since steady-state calculations are incapable of capturing unsteady effects, the forces in these simulations are based on reproducing the deformation in the unsteady simulations (*i.e.* equivalent loads). These equivalent loads are based on unsteady DLC simulations in the upper level. When the optimization at the lower level finds a solution, the upper level calculations are performed to re-calibrate the equivalent loads. This process repeats until convergence.

Steady-state analysis is not the only simplification used in optimization. Merz⁶ and Tibaldi⁷ independently developed a frequency domain approach to evaluating the fatigue loads. This is an extension of steady-state analysis, where a steady state solution is required, then the system is linearized about this steady state solution. A first order estimate of the structural estimate can be estimated with a matrix multiplication of the linear system and a Fourier series of the inflow in the blade reference frame. Compared to full unsteady simulations, this is an inexpensive approach to incorporating unsteady effects within the optimization framework.

Since feasibility is more important than optimality, these simplifications are tuned to be conservative. In these cases the feasible region seen by the optimization algorithm is smaller than the true feasible region. Solutions to constrained optimization problems typically lie on the boundary of the feasible region, thus, these approximations lead to sub-optimal designs. Figure 1 demonstrates this point graphically with a hypothetical problem.

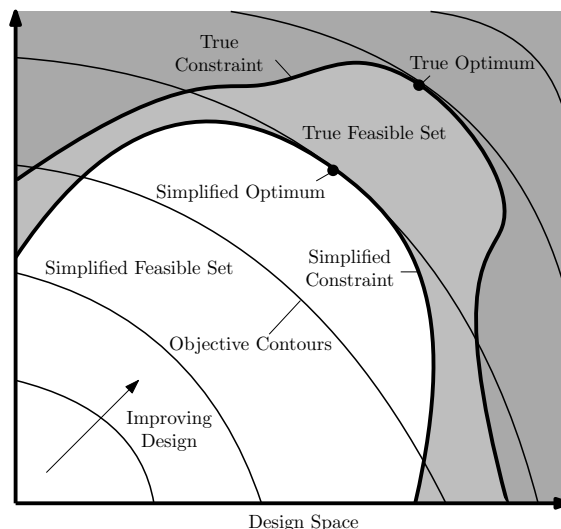


Figure 1: Effect of simplified constraints

Many of the frameworks presented in literature rely on steady-state analysis as a simplification. In these cases the optimization would be blind to unsteady aero-elastic effects during various extreme gust scenarios. Since these load cases are driving for many designs, this limitation would conceal beneficial aero-elastic designs or serious problems.

A second and maybe more important driver for higher fidelity optimization is the fact that it is required to properly assess advanced turbine concepts. Examples are turbines with winglets, active flaps, bend-twist coupling and many other concepts. It is not always clear how these innovations will have maximum impact on the design. For example load alleviation strategies could improve Annual Energy Production (AEP) with larger rotors or yield lighter less expensive turbines. Optimization is an ideal tool for evaluating these trade-off's and finding the best application of these different innovations.

To capture the boundaries of the true feasible region, or the impact of advanced turbine concepts, higher fidelity analysis is required in the optimization. Yet, performing direct optimization on higher fidelity analysis is prohibitively expensive and challenging. This research will explore multi-fidelity optimization techniques to improve the fidelity in optimization, while keeping the optimization reasonably efficient. Section II gives a brief description of the Approximation and Model Management Framework (AMMF) algorithm. Then section III will outline the optimization and analysis tools that will be used in this framework. Then in section IV several case studies on the AMMF algorithm are given.

II. Multi-fidelity optimization techniques

The problem of incorporating expensive high-fidelity simulation methods within optimization is not a new problem. The aerospace literature gives many such examples.⁸⁻¹² The basic approach is to use a fast low-fidelity model in place of the expensive simulation within the optimization. The expensive simulation is used just to train and correct the surrogate model. This basic approach bears some similarity to techniques of other wind turbine optimization frameworks,^{1,5} the differences lie in approximation methods and how the low and high fidelity models are used to construct and update the surrogate. The research in this paper will focus on the AMMF algorithm.

In wind turbine analysis, multiple fidelities could come in many forms. First, the traditional interpretation is the use of multiple grid spacing with the same analysis methods. Second, multi-fidelity could be different formulations of the same physical phenomenon. One example in aerodynamics is BEM, then Lagrangian Vortex Dynamics (LVD) and finally grid based Computational Fluid Dynamics (CFD) codes like ellipsis.

The multitude of simulations required in evaluating the DLCs provides another opportunity for multi-fidelity. Simulating the full DLC represents the high fidelity approach, then lower fidelity version are achieved by using a reduced DLC. The DLCs can be reduced by simulating only the most important DLCs. Further reductions can be achieved by ignoring the stochastic effects of turbulence with fewer turbulence seeds.

II.A. Approximation and Model Management Framework

One attractive multi-fidelity approach is given by Alexandrov *et. al.* called Approximation and Model Management Framework (AMMF).¹³ It is a general approach that assumes there is an expensive high fidelity simulation and a fast low fidelity approximation. The goal is to find the optimal solution for the high fidelity response, yet save computational time by performing the search with the low fidelity analysis (see figure 2). This approach is similar to that of Fuglsang *et. al.* and Bottasso *et. al.*, but AMMF differs in 2 ways. First the low fidelity simulation (f_l) is corrected with either a multiplicative correction (equation (1a)) or an additive correction (equation (1b)), where \tilde{f} is the corrected response of the low-fidelity solution, β is the correction, which are all functions of the design vector \mathbf{x} . The corrected response is made equivalent to the high-fidelity response $f_h(\mathbf{x})$ in both the value (*i.e.* $\tilde{f}(\mathbf{x}_0) = f_h(\mathbf{x}_0)$) and the gradient (*i.e.* $\nabla \tilde{f}(\mathbf{x}_0) = \nabla f_h(\mathbf{x}_0)$) at the reference point \mathbf{x}_0 using the correction in equation (1c) for β_m or equation (1d) for β_a .

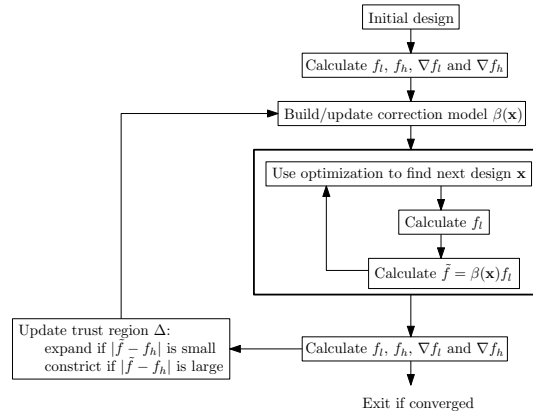


Figure 2: The AMMF algorithm

$$\tilde{f}(\mathbf{x}) = \beta_m(\mathbf{x})f_l(\mathbf{x}) \quad (1a) \quad \tilde{f}(\mathbf{x}) = f_l(\mathbf{x}) + \beta_a(\mathbf{x}) \quad (1b)$$

$$\beta_m(\mathbf{x}) = \left(\frac{f_h(\mathbf{x}_0)}{f_l(\mathbf{x}_0)} \right) + \left(\frac{\nabla f_h(\mathbf{x}_0) \cdot (\mathbf{x} - \mathbf{x}_0)}{f_l(\mathbf{x}_0)} - \frac{f_h(\mathbf{x}_0)\nabla f_l(\mathbf{x}_0) \cdot (\mathbf{x} - \mathbf{x}_0)}{f_l^2(\mathbf{x}_0)} \right) \quad (1c)$$

$$\beta_a(\mathbf{x}) = (f_h(\mathbf{x}_0) - f_l(\mathbf{x}_0)) + (\nabla f_h(\mathbf{x}_0) \cdot (\mathbf{x} - \mathbf{x}_0) - \nabla f_l(\mathbf{x}_0) \cdot (\mathbf{x} - \mathbf{x}_0)) \quad (1d)$$

Second, a trust region is employed to prevent errors in the low-fidelity model taking the optimization away from the high-fidelity minimum. Since the approximation is only based on local information, it will only give acceptable estimates close to the reference point. To prevent the optimization from moving into regions with poor approximations, the inner optimization is constrained to stay within a trust region (through boundary constraints). When the inner optimization finds a suitable solution, the trust region is re-centered on that solution and possibly resized. Then another approximation is constructed and the inner optimization proceeds in the new trust region. Figure 3 shows a hypothetical example of this where the colored squares are the trust regions for different iteration of the AMMF algorithm and the red line shows the optimization progress starting from the bottom left.

Extending the multi-fidelity approach to the constraints is an important aspect of wind turbine design engineering. In this research the constraints are corrected in the same way as the objective using equations (1). The constraints are incorporated into the AMMF algorithm by using the Lagrangian shown in equation (2), where \mathbf{g}_e and \mathbf{g}_i are the equality and inequality constraint respectively and $\tilde{\lambda}_e$ and $\tilde{\lambda}_i$ are the respective Lagrange multipliers. These Lagrange multipliers are estimated from the high fidelity gradient information

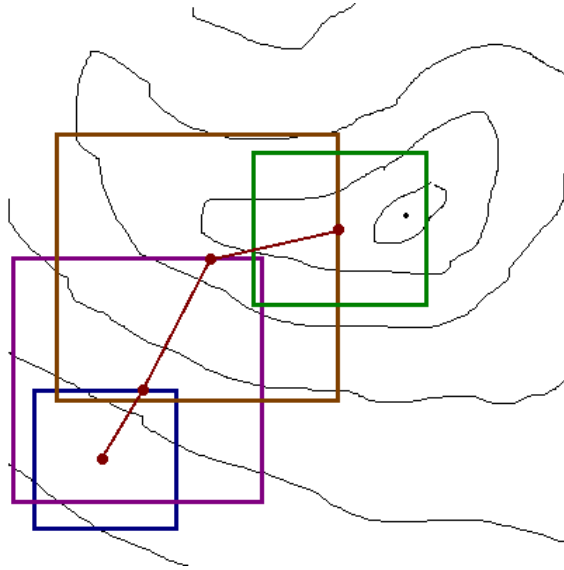


Figure 3: Example of the trust region algorithm

from the most recent gradient information. Since, at the initial stages when not all constraints are active, the Lagrange multipliers may be zero. To avoid this the minimum Lagrange multiplier is specified by the user. The merit of the inner optimization solution is based on improving Φ . Similarly Φ is used in equation (3) to calculate the merit M of the approximation. That information is used to either expand, contracts or maintain the trust region size, depending on how far it is from 1. In this work the trust region was doubled in size if M was between 0.75 and 1.25, or contracted to half the original size if it was under 0.1.

$$\Phi = f_h + \tilde{\lambda}_e^T |g_e| + \tilde{\lambda}_i^T \max(\mathbf{0}, g_i) \quad (2)$$

$$M = \frac{\Phi_{i-1} - \Phi_i}{\Phi_{i-1} - \tilde{\Phi}_i} \quad (3)$$

III. Optimization and analysis tools

These algorithms have been incorporated into the DTU HAWTOpt2 optimization framework for wind turbine design optimization.¹⁴ The framework incorporates HAWC2¹⁵ and HAWCStab2¹⁶ for evaluating the aero-elastic loads of a wind turbine and BEam Cross section Analysis Software (BECAS)¹⁷ for the cross section properties. The framework relies on the OpenMDAO¹⁸ package to couple all these simulation codes together with a variety of optimization algorithms. Finally the Dakota toolkit¹⁹ is also used for the optimization and parameter tuning.

To explore multi-fidelity optimization, some low fidelity tools have been developed in C++ by the author. The first is a cross section analysis tool based on thin walled cross section assumptions, Classical Laminate Theory (CLT) and rigid cross section assumption. Table 1 shows the relative error compared to BECAS for evaluating the DTU 10MW blade.

As an alternative to the nonlinear multi-body formulation used in HAWC2 and HAWCStab2 the author has developed a simple linear beam model based on standard textbook formulations.²⁰ This beam model includes analytic gradients with respect to the initial shape, orientation, material properties and the force distribution.

Table 2 gives the computational times of all these tools in calculating the deflection of the DTU 10MW wind turbine under static loading. These tools are ideal for exploring multi-fidelity techniques due the relatively small differences in accuracy (*i.e.* table 1) and the large disparity in simulation time (*i.e.* table 2).

Table 1: Relative error of the low-fidelity cross section model with BECAS

Position	EA	EI_x	EI_y	GJ
0.05	0.0%	2.6%	-4.9%	-5.4%
0.15	0.5%	1.1%	-3.0%	-0.8%
0.25	-0.4%	-1.8%	2.1%	-1.4%
0.35	-0.7%	-2.6%	1.7%	-3.1%
0.45	-0.7%	-3.1%	1.0%	-5.5%
0.55	-0.9%	-3.1%	-0.3%	-7.7%
0.65	-0.8%	-2.9%	-1.7%	-9.3%
0.75	-0.6%	-2.2%	-2.2%	-9.2%
0.85	-0.6%	-1.7%	-3.5%	-5.9%
0.95	-0.1%	-1.2%	-2.0%	-2.0%

Table 2: Speed Comparison of Low Fidelity Tools

Operation	Calculation time [s]
Linear beam model	0.0035
Low-fidelity cross section model	0.0074
BECAS	200.1866

IV. Optimization Studies

Three optimization studies were conducted in this research. First a simple analytic problem was used to explore the efficacy of the AMMF algorithm with varying levels of error. The next studies looked at applying these techniques on a variety of physical models. The DTU 10MW reference wind turbine design²¹ was used as the reference case. The first study focused on simple single disciplinary optimization problems as described in section IV.B. The ultimate goal of this research is to develop improved MDO techniques for wind turbines, section section IV.C presents the first attempt of applying AMMF on a full rotor design problem.

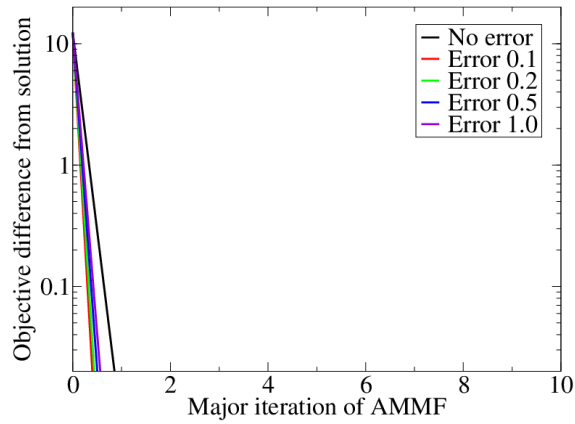
IV.A. Preliminary investigation

This study was conducted to see how AMMF will handle different errors between the low-fidelity and the high-fidelity models. Here, the basic problem is a paraboloid as shown in equation (4). Then to investigate the effect of the error, the same paraboloid was offset with various polynomial offsets to create a hypothetical low-fidelity representation of the original function.

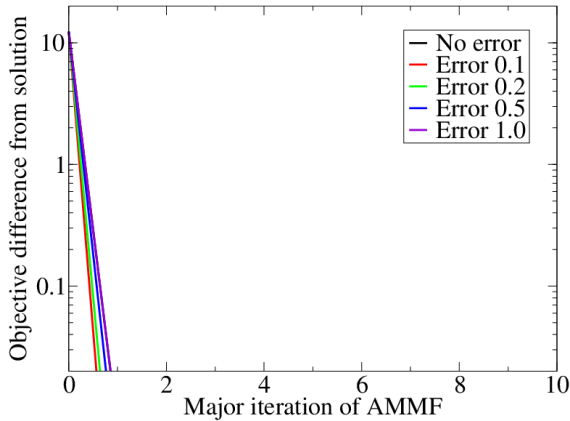
$$z = (x - 3)^2 + (y + 4)^2 + xy + 300 \quad (4)$$

Figure 4 show the effect of constant offset error, linear error and quadratic error. In each case the optimal solution of the synthetic low-fidelity problem is the same as the original high-fidelity problem (i.e. the error is 0 at the optimal solution). The AMMF correction ensures C^1 consistency between the low and high fidelity responses. The results in figure 4a and 4c shows this correction makes AMMF insensitive to constant and linear offset errors. However, figure 4c shows quadratic errors (and presumably higher order errors) require the correction to be updated several times to converge to the solution. Thus the remainder of the study looked at the effects of quadratic error.

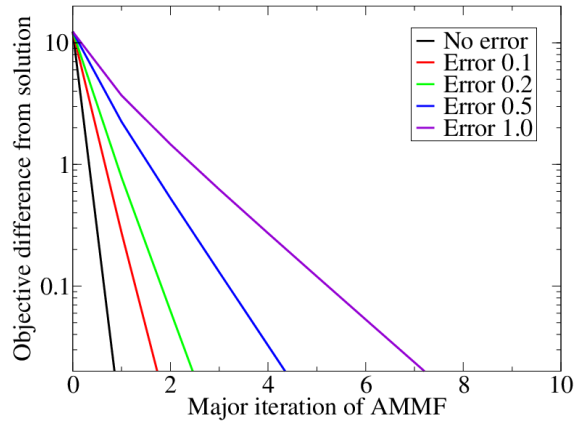
The position of the local minimum in the low fidelity model could also have an effect on the performance. To explore this effect, the offset polynomial was centered either far behind the starting point or far beyond the optimal solution. In the former case the low-fidelity problem will tend to under-shoot the problem and over-shoot in the other case. These synthetic low-fidelity responses are shown figure 5a along a line in the design space that passes through the starting point and the optimal solution. The distance in the design



(a) Constant offset error



(b) Linear offset error



(c) Quadratic offset error

Figure 4: The effect of error in the low-fidelity model on AMMF convergence

space has been normalized so the starting point in the optimization is at 0, and the optimal solution for the high-fidelity problem is at 1.

Figure 5b shows that over and under shoot has a positive effect on the convergence. When over or under shoot is present the trust region must be constricted to maintain good convergence. It seems that the trust region becomes tuned to the optimal search length for the optimization. However, this tuning requires additional high fidelity solutions. Figure 5c shows that severe differences between the high and low fidelity models require many more high-fidelity function evaluations to achieve good convergence. This shows that in the worst case, AMMF starts to behave more like direct optimization with the high-fidelity simulation. Thus, the algorithm is robust.

IV.B. Single discipline investigations

A common application in wind turbine design optimization is in the design of the internal structure. One approach is to perform a set of aeroelastic calculations on a design. The results of this calculation define the loading on the blade. Then optimization is used to find the structure with the minimum weight that can withstand these loads. By assuming the aero-elastic loads are constant, the optimization only required Finite Element Method (FEM) analysis of the internal structure. Additional aero-elastic calculations would have to be performed as the design evolves to update the loads.

The AMMF algorithm was applied to this problem. The high fidelity model was based on BECAS¹⁷ for the cross section stiffness properties and linear beam model for the deflection. The low fidelity model is based on CLT for the cross section stiffness properties and the same linear beam model for the deflection.

Results from a full DLC evaluation were used to determine the deformed state of the blade when the maximum tip deflection occurred. Then an inverse problem was solved to determine the equivalent static

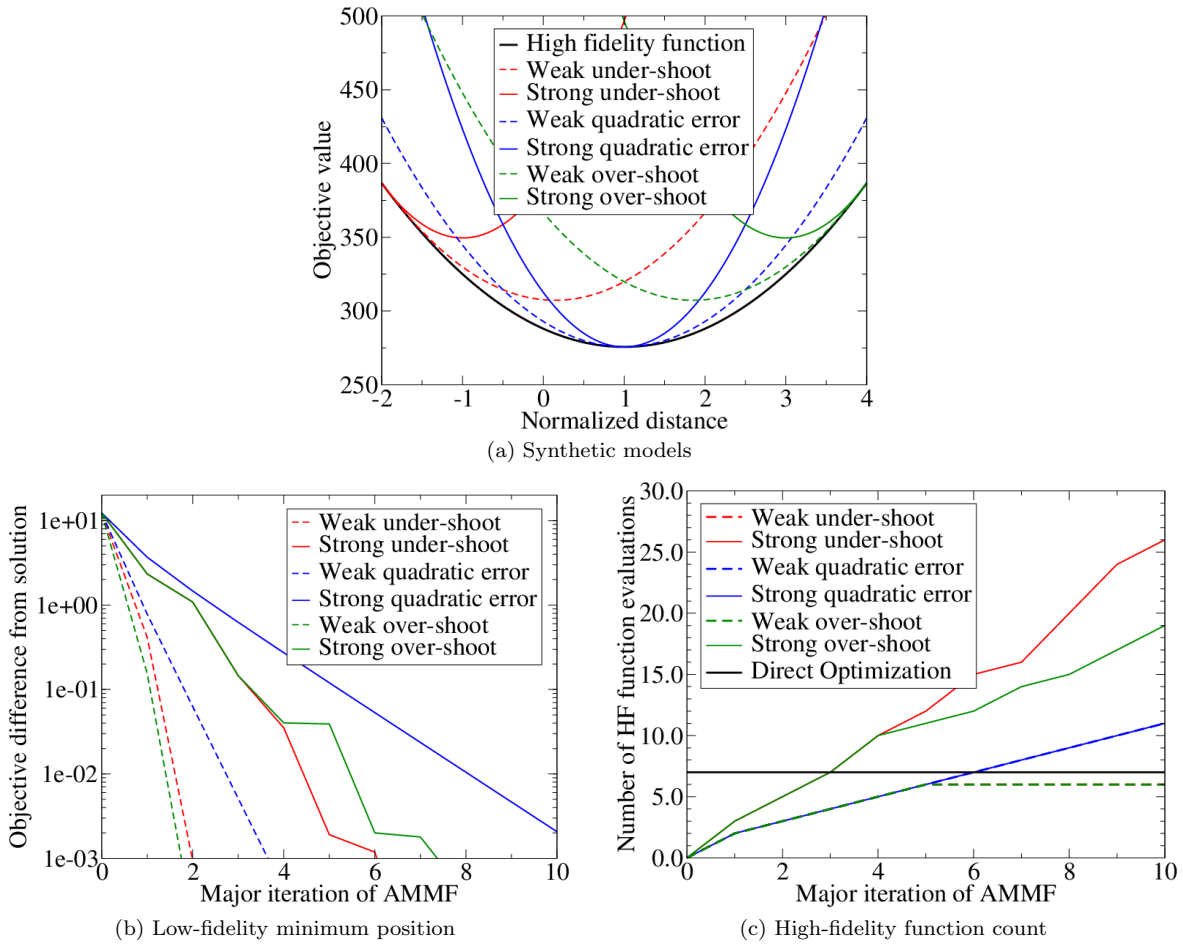


Figure 5: Effect of minimum location on AMMF convergence

loads to achieve the equivalent deformed state. The goal of the design optimization was to minimize the weight of blade by varying the spar-cap thickness without increasing the tip deflection when subjected to these loads. Gradient based optimization was used to solve this problem, finite difference gradients were used in all cases.

Figure 6 shows the optimization results. AMMF was compared with direct optimization with both CLT and BECAS. The results show that optimization based on CLT is not conservative and would lead to unsafe designs. Thus, one would have to apply larger safety factors which in-turn would lead to sub-optimal designs. AMMF managed to achieve identical results as direct optimization with BECAS. Thus, it was successful in incorporating the extra high-fidelity information to achieve a feasible and optimal design.

Figure 7 shows the progress of the AMMF algorithm in comparison with direct optimization with BECAS. It is clear that AMMF was able to converge the results much fast than with BECAS. In this example AMMF converged in 2 outer iterations, while direct BECAS required approximately 30 iterations. This shows that only a small amount of high-fidelity information is required to achieve equivalent results.

The first order correction in AMMF introduces increasing error moving away from the reference point. To compensate for this error the AMMF algorithm employs 2 features. First, a trust region is used so the optimization stays within a domain where the approximation is acceptable. Second, the Lagrange multipliers are used to penalize constraint violations when the AMMF algorithm evaluates whether an optimization solution should be accepted or not.

This problem was used to explore how these features improve the robustness of the optimization. Figure 8 shows how the optimization fails to converge when both of these features are disabled. Since CLT is not conservative the optimization makes a large jump into an infeasible region and cannot recover. Each of the robustness features was enabled and in both cases the optimization was able to converge. The results show that only one of these features needs to be enabled to achieve robust convergence. Thus, if the user does

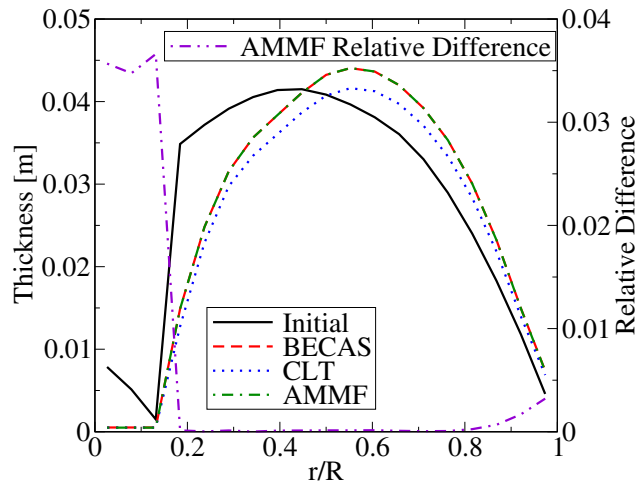


Figure 6: Structural Optimization Results

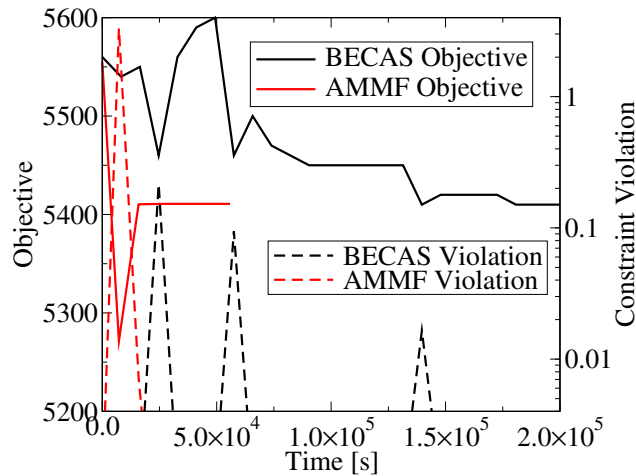


Figure 7: Structural Optimization Progress

not know a suitable initial trust region they can use a large initial penalty. Otherwise if a good initial trust region is known, then the initial penalty is not important and can be set to a small value and subsequently calculated by the AMMF algorithm.

Both additive and multiplicative corrections were applied in this study. Both corrections gave similar results and show no significant advantage.

IV.C. Multi-disciplinary design optimization

The final case study attempted to perform full aero-elastic design optimization on a wind turbine rotor. The design focused on maximizing the AEP, subject to extreme loads, fatigue, rotor thrust and tip deflection constraints. The optimization varied planform design variables (chord, twist, relative thickness and rotor radius) along with internal structural variables (laminate thickness, web and spar-cap positioning). This test case uses the HAWTOpt2 optimization framework which includes BECAS for the cross section analysis, HAWCStab2 for steady state analysis and HAWC2 for unsteady calculations. HAWCStab2 is used to evaluate the AEP and the operational C_l . While HAWC2 is used to evaluate only a subset of the DLC to determine the extreme loads.

Typically HAWC2 is the most expensive component in the work flow. A low fidelity version of this workflow was created by using the steady state loads calculated from HAWCStab2 in place of the loads from HAWC2. These steady state loads ignore the effect of turbulence, so they were increased with a dynamic amplification factor. The optimal dynamic amplification factor should reproduce similar loads as a full

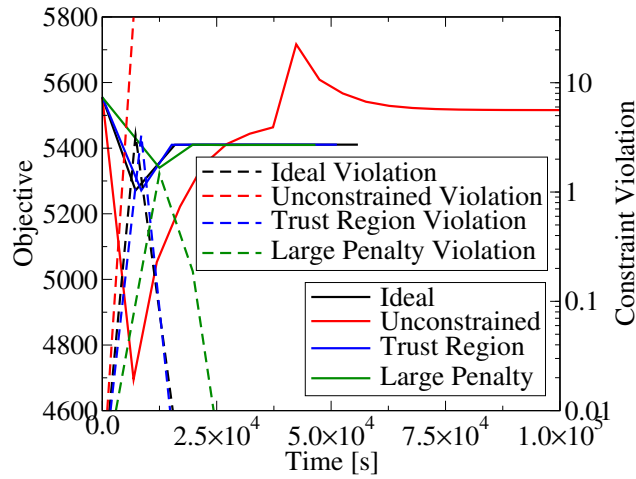


Figure 8: Robustness of the AMMF Algorithm

DLC. The parameter tuning routines of DAKOTA¹⁹ were used to determine the best amplification factors to approximate a full DLC load envelope. Figure 9 shows how this steady state model compares with full unsteady results. This steady state analysis ignores dynamic effect and thus, these amplification factors would have to be re-tuned as the design evolves. However, they were held constant throughout the rest of the study.

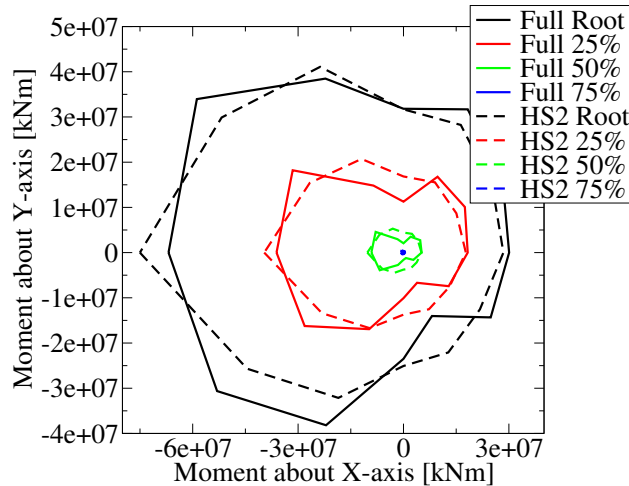


Figure 9: Comparison of load envelopes

The AMMF algorithm was applied to correct this work-flow. The goal was to reproduce the results of direction optimization with HAWC2. In this work-flow only one component was replaced with a low-fidelity equivalent, the remaining components were the same in both the low-fidelity and high fidelity work-flows. Since the two work-flows shared many of the same components the overall execution time was similar. Accordingly, the AMMF algorithm was significantly slower and fully converged results could not be achieved with AMMF within the time limit of the computational facilities. This shows that a multi-fidelity approach only provides advantages when there is a significant difference in execution time between the two work-flows.

Figure 10 shows the chord solution after one iteration of the AMMF algorithm. This solution is compared to the final solution of direct optimization of the original HAWC2 based work-flow. This result shows that AMMF is approaching the direction optimization solution. Despite the poor computational performance the AMMF algorithm is approaching the expected solution. AMMF was only applied to this pair of work-flows, further improvements could be achieved by incorporating either faster low-fidelity models or higher fidelity models. Further work is needed to determine the set of models where AMMF provides an advantage in design optimization.

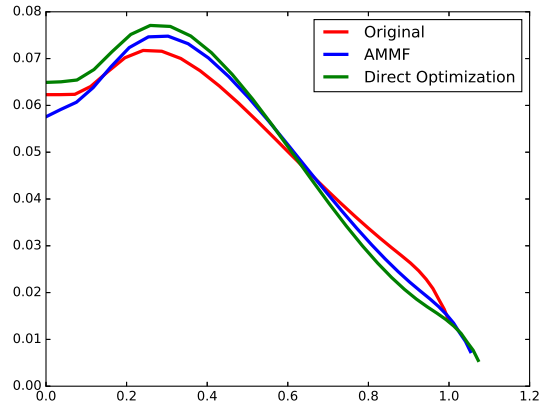


Figure 10: Chord Solutions

The AMMF correction was applied to the objective and all the constraint values. Some of these values were close to zero. In these circumstances only the additive correction gave good results.

V. Conclusions

Calculating the full set of DLCs for a wind turbine is too expensive within optimization. This means many examples of design optimization in literature rely on either powerful computing facilities, or some form of simplified analysis. In the case of simplified approaches, the optimization could lead to sub-optimal designs. An attractive alternative is to apply multi-fidelity design optimization. This paper looked at the AMMF algorithm for a variety of wind turbine rotor design problems.

First, this paper evaluated how AMMF performed with different levels of error in the optimization of a simple analytic problem. Overall, increasing error had a detrimental effect on the computational performance, but AMMF proved to be robust at converging towards the high-fidelity solution.

Second, the AMMF algorithm was applied to a structural design optimization problem. Here, the low fidelity model was significantly faster and produced similar results as the high-fidelity model. Here, AMMF was able to converge the optimization significantly faster than direct optimization with the high fidelity model. Furthermore the converged results were identical to the direct high fidelity optimization results.

The AMMF algorithm explored in this work uses both a trust region and penalty functions to mitigate problems due to the error in the low-fidelity model. This study shows that only one of these features is needed to achieve robust performance with AMMF.

Finally, AMMF was applied to an aero-elastic rotor design problem. The execution time of the low fidelity model was still significant compared to the high-fidelity model. Thus, the extra complexity of the AMMF algorithm lead to slower over-all convergence. The results show AMMF was approaching the high-fidelity solution. Only one pair of models were explored, thus, more work is needed to find a suitable mix of low and high fidelity models where AMMF will provide an advantage to rotor design optimization.

References

- ¹Fuglsang, P. and Madsen, H. A., "Optimization method for wind turbine rotors," *Journal of Wind Engineering and Industrial Aerodynamics*, Vol. 80, 1999, pp. 191–206.
- ²Hansen, M. H., Thomsen, K., Natarajan, A., and Barlas, A., "Design Load Basis for onshore turbines - Revision 00," Tech. rep., Danish Technical University, 2015.
- ³IEC, "IEC 61400-1 Wind turbines - Part 1: Design Requirements Third Edition," Tech. rep., International Electrotechnical Commission, 2005.
- ⁴Hjort, S., Dixon, K., Gineste, M., and Olsen, A. S., "Fast Prototype Blade Design," *Wind Engineering*, Vol. 33, 2009, pp. 321–334.
- ⁵Bottasso, C., Campagnolo, F., and Croce, A., "Multi-disciplinary constrained optimization of wind turbines," *Multibody System Dynamics*, Vol. 27, No. 1, 2012, pp. 21–53.

⁶Merz, K. O., “Rapid optimization of stall-regulated wind turbine blades using a frequency-domain method: Part 2, cost function selection and results,” *Wind Energy*, Vol. 18, No. 6, 2015, pp. 955–977.

⁷Tibaldi, C., *Concurrent Aeroservoelastic Design and Optimization of Wind Turbines*, Ph.D. thesis, Danish Technical University, 2015.

⁸Koziel, S., Ciaurri, D. E., and Leifsson, L., “Surrogate-Based Methods,” *Computational Optimization, Methods and Algorithms - State of the art in Computational Optimization*, edited by S. Koziel and X.-S. Yang, Vol. 356, chap. 3, Springer-Verlag Berlin Heidelberg, 1st ed., 2011, pp. 33–59, ISBN: 978-3-642-20859-1.

⁹Forrester, A. I. and Keane, A. J., “Recent advances in surrogate-based optimization,” *Progress in Aerospace Sciences*, Vol. 45, No. 13, 2009, pp. 50 – 79.

¹⁰Queipo, N. V., Haftka, R. T., Shyy, W., Goel, T., Vaidyanathan, R., and Tucker, P. K., “Surrogate-based analysis and optimization,” *Progress in Aerospace Sciences*, Vol. 41, No. 1, 2005, pp. 1 – 28.

¹¹Simpson, T., Toropov, V., Balabanov, V., and Viana, F., “Design and Analysis of Computer Experiments in Multidisciplinary Design Optimization: A Review of How Far We Have Come - Or Not,” *Multidisciplinary Analysis Optimization Conferences*, American Institute of Aeronautics and Astronautics, Sept. 2008, pp. –.

¹²Simpson, T., Booker, A., Ghosh, D., Giunta, A., Koch, P., and Yang, R.-J., “Approximation methods in multidisciplinary analysis and optimization: a panel discussion,” *Structural and Multidisciplinary Optimization*, Vol. 27, No. 5, 2004, pp. 302–313.

¹³Alexandrov, N. M., Lewis, R. M., Gumbert, C. R., Green, L. L., and Newman, P. A., “Approximation and Model Management in Aerodynamic Optimization with Variable-Fidelity Models,” *Journal of Aircraft*, Vol. 38, No. 6, Nov. 2001, pp. 1093–1101.

¹⁴Zahle, F., Tibaldi, C., Verelst, D., Bak, C., Bitsche, R., and Blasques, J., *Aero-Elastic Optimization of a 10 MW Wind Turbine*, Vol. 1, American Institute of Aeronautics & Astronautics, 2015, pp. 201–223.

¹⁵DTU Wind Energy, “HAWC2,” <http://www.hawc2.dk>, Accessed: 2016-06-06.

¹⁶DTU Wind Energy, “HAWCStab2,” <http://www.hawcstab2.vindenergi.dtu.dk>, Accessed: 2016-06-06.

¹⁷Blasques, J., Bitsche, R., Fedorov, V., and Lazarov, B., “Accuracy of an efficient framework for structural analysis of wind turbine blades,” *Wind Energy*, 2015.

¹⁸Gray, J., Moore, K. T., Hearn, T. A., and Naylor, B. A., “Standard Platform for Benchmarking Multidisciplinary Design Analysis and Optimization Architectures,” *AIAA Journal*, Vol. 51, No. 10, Oct 2013, pp. 2380–2394.

¹⁹Sandia National Laboratories, “Dakota - Algorithms for design exploration and simulation credibility,” <https://dakota.sandia.gov>, Accessed: 2016-06-06.

²⁰Logan, D. L., *A First Course in the Finite Element Method Fourth Edition*, Thomson, 1120 Birchmount Road, Toronto, Ontario, M1K 5G4 Canada, 2007.

²¹Bak, C., Zahle, F., Bitsche, R., Kim, T., Yde, A., Henriksen, L., Hansen, M., Blasques, J., Gaunaa, M., and Natarajan, A., “The DTU 10-MW Reference Wind Turbine,” *Danish Wind Power Research*, 2013.